www.elsevier.com/locate/yexcr

Involvement of PUMA in pericyte migration induced by methamphetamine

Yanhong Zhang, Yuan Zhang, Ying Bai, Jie Chao, Gang Hu, Xufeng Chen, Honghong Yao

PII: S0014-4827(17)30218-5
DOI: http://dx.doi.org/10.1016/j.yexcr.2017.04.007
Reference: YEXCR10570

To appear in: *Experimental Cell Research*

Received date: 17 February 2017
Revised date: 6 April 2017
Accepted date: 8 April 2017

Cite this article as: Yanhong Zhang, Yuan Zhang, Ying Bai, Jie Chao, Gang Hu, Xufeng Chen and Honghong Yao, Involvement of PUMA in pericyte migration induced by methamphetamine, *Experimental Cell Research* http://dx.doi.org/10.1016/j.yexcr.2017.04.007

Involvement of PUMA in pericyte migration induced by methamphetamine

Yanhong Zhang[1], Yuan Zhang [1], Ying Bai[1], Jie Chao[2], Gang Hu[3], Xufeng Chen[4*] , Honghong Yao[1, 5]*

[1]Department of Pharmacology, Medical School of Southeast University, Nanjing, China

[2]Department of Physiology, Medical School of Southeast University, Nanjing, China

[3]Department of Pharmacology, Nanjing Medical University, Nanjing, China

[4]Department of Emergency, Jiangsu Province Hospital, Nanjing, Jiangsu, China

[5]Institute of Life Sciences, Key Laboratory of Developmental Genes and Human Disease, Southeast University, Nanjing, Jiangsu, China

Yanhong Zhang, E-mail: zhangyanhong@seu.edu.cn

Yuan Zhang, Ph.D. E-mail: yuanzhang@seu.edu.cn

Ying Bai, M.D. E-mail: yingbai@seu.edu.cn

Jie Chao, Ph.D. E-mail: chaojie@seu.edu.cn

Gang Hu, Ph.D. E-mail: ghu@njmu.edu.cn

E-mail: cxfyx@163.com

E-mail: yaohh@seu.edu.cn

*__Corresponding Author:__ Xufeng Chen Department of Emergency, Jiangsu Province Hospital, Nanjing, Jiangsu, China 210029

*__Corresponding Author:__ Honghong Yao, Ph.D. Department of Pharmacology,

Medical School of Southeast University, Nanjing, Jiangsu, China 210009, Tel: 86-25-83272551

Abstract

Mounting evidence indicates that methamphetamine causes blood-brain barrier damage, with emphasis on endothelial cells. The role of pericytes in methamphetamine-induced BBB damage remains unknown. Our study demonstrated that methamphetamine increased the migration of pericytes from the endothelial basement membrane. However, the detailed mechanisms underlying this process remain poorly understood. Thus, we examined the molecular mechanisms involved in methamphetamine-induced pericyte migration. The results showed that exposure of C3H/10T1/2 cells and HBVPs to methamphetamine increased PUMA expression via activation of the sigma-1 receptor, MAPK and Akt/PI3K pathways. Moreover, methamphetamine treatment resulted in the increased migration of C3H/10T1/2 cells and HBVPs. Knockdown of PUMA in pericytes transduced with PUMA siRNA attenuated the methamphetamine-induced increase in cell migration through attenuation of integrin and tyrosine kinase mechanisms, implicating a role of PUMA in the migration of C3H/10T1/2 cells and HBVPs. This study has demonstrated that methamphetamine-mediated pericytes migration involves PUMA up-regulation. Thus, targeted studies of PUMA could provide insights to facilitate the development of a potential therapeutic approach for alleviation of methamphetamine-induced pericyte migration.

Graphical abstract

Exposure of pericytes to methamphetamine leads to activation of the MAPK and PI3K/Akt pathways, with downstream activation of PUMA, leading to enhanced pericyte migration. Knockdown of PUMA expression inhibited integrin β1 and β3 expression, as well as tyrosine kinase phosphorylation, and subsequently decreased pericyte migration.

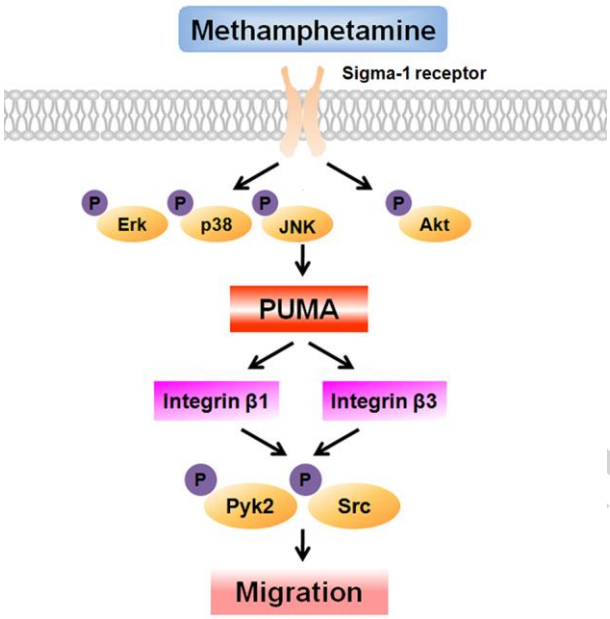

Abbreviations

ALS: Amyotrophic lateral sclerosis; BBB: Blood-brain barrier; BMECs: Brain microvascular endothelial cells; CNS: Central nervous system; HBVPs: Human brain vascular pericytes; MAPK: Mitogen-activated protein kinase; MS: Multiple sclerosis; MTT: 3-[4,5-dimethylthiazol-2yl]-2,5-diphenyltetrazoliumbromide; NGS: Normal goat serum; OD: Optical density; PBS: Phosphate-buffered saline; PI3K: phosphatidylinositol-3' kinase; PVDF: Polyvinylidene fluoride; RT: Room temperature; PUMA: P53 up-regulated modulator of apoptosis; SDS-PAGE: Sodium dodecyl sulfate-polyacrylamide gel electrophoresis; TBST: Tris-buffered saline with Tween-20; TJP: Tight junction protein.

Keywords: PUMA; Methamphetamine; C3H/10T1/2 cells; migration

Introduction

The blood-brain barrier (BBB) is a dynamic network that helps to maintain central nervous system (CNS) homeostasis by restricting the passage of toxic substances into the brain. Brain microvascular endothelial cells (BMECs) are the basic components of the BBB and play a critical role in maintaining its integrity under physiological conditions [1-4]. BBB dysfunction has been demonstrated in various neurological disorders, including stroke, Alzheimer's disease, and epilepsy, as well as in drug abuse [5-7], which is a major social and health concern. Methamphetamine is a popular addictive pharmacological CNS psychostimulant, and its use is associated with multiple adverse neuropsychiatric reactions, as well as with neurotoxicity to the dopaminergic and serotonergic systems in the brain [8, 9].

Methamphetamine exposure *in vivo* has been shown to disrupt the BBB [10-13]. Disruption of BBB integrity is not only a common consequence of methamphetamine-induced neuroinflammation[14], but it also contributes to its progression. Protection of the cerebral endothelium is an important therapeutic goal in methamphetamine-induced BBB damage. Although much is known about the devastating effects of methamphetamine on endothelial cells[15, 16] and glial function[17], its effects on brain pericytes remain largely under-characterized. Pericytes are necessary for formation of the BBB[18], and the absolute pericyte coverage determines the relative vascular permeability[19]. Pericyte versatility is largely unexplored, but several studies

have suggested that pericytes may play roles in brain repair through contractile, migratory, proangiogenic and phagocytic functions and that the responses of these cells to toxins may also promote brain impairment[20]. Under normal conditions, the morphological pattern of pericyte projections around brain capillaries is linked to their function. This classic wrapping pattern consists of broad processes with a large continuous surface in the external walls of brain microvessels. However, under pathological conditions, detachment and migration patterns have been observed with the formation of finger-like projections, followed by retraction of the projections[21]. These data suggest that pericytes play important roles in maintaining the integrity and function of the BBB and that they may thus represent a novel therapeutic target in many diseases. However, little is known about pericyte dysfunction during methamphetamine exposure.

P53 up-regulated modulator of apoptosis (PUMA) is a member of the BH3-only subgroup of the Bcl-2 family. It is a critical mediator of p53-dependent and p53-independent apoptosis and exerts strong pro-apoptotic effects [22, 23]. Emerging evidence suggests that PUMA acts as a proangiogenic factor to promote cell proliferation and survival and that it has therapeutic potential in treating cancer and degenerative diseases[24]. Our previous study has indicated that knockdown of PUMA attenuates the increased fibroblast proliferation and migration in silicosis. However, whether PUMA is involved in methamphetamine-induced pericyte migration remains

unknown.

Thus, the present study sought to determine whether PUMA is involved in methamphetamine-induced pericyte migration. We have provided direct evidence that methamphetamine induces pericyte migration, thereby contributing to BBB damage in drug abusers via a previously unidentified role of PUMA.

Material and methods

Cell culture

Primary human brain vascular pericytes (HBVPs) were purchased from ScienCell (Carlsbad, CA, USA) and cultured in pericyte medium (provided by ScienCell). Cells were incubated in a CO_2 incubator (Thermocon Electron Corporation, Waltham, MA, USA) at 37 °C in a humidified atmosphere of 5 % CO_2 and 95 % air, and they were used at passages 2-8. The pericyte cell line C3H/10T1/2, clone 8, was purchased from the American Type Culture Collection (CCL226). Cells were grown in Eagle's Minimum Essential Medium (EMEM) containing 10 % heat-inactivated fetal bovine serum and 1 % penicillin/streptomycin, and they were used at passages 4-14.

Reagents

Methamphetamine was purchased from the National Institute for the Control of Pharmaceutical and Biological Products (Beijing, China). The

specific MEK1/2 inhibitor U0126, JNK inhibitor SP60012, p38 inhibitor SB203580, and phosphatidylinositol-3' kinase (PI3K) inhibitor LY294002 were purchased from Calbiochem (San Diego, CA, USA). A sigma receptor antagonist, BD1047, was obtained from Sigma-Aldrich (St. Louis, MO, USA). LEAF purified anti-mouse/rat CD29 (neutralizing β1 antibody; clone HM β1-1) and LEAF purified anti-mouse/rat CD61 (neutralizing β3 antibody; clone 2c9.G2; HM β3-1) were purchased from BioLegend (San Diego, CA, USA). Purified rabbit IgG was obtained from Millipore (Merck, Darmstadt, Germany). The concentrations of these inhibitors were based on concentration-curve analysis and our previous reports [25].

MTT assay

Cell viability was examined using the MTT assay as described previously [26]. Cells were seeded in a 96-well plate and were then treated with 100 μM methamphetamine. After 24 h of methamphetamine exposure, MTT dye was added at 1 h before termination of the experiment. Optical density (OD) was measured at 570 nm using a Synergy H1 Multi-Mode Reader (BioTek, Winooski, VT, USA).

Immunofluorescence staining

Pericytes (HBVPs and C3H/10T1/2 cells) were cultured on coverslips coated with poly-D-lysine (0.05 mg/ml; Sigma, St. Louis, MO). After 30 min or 3

h of exposure to methamphetamine, the cells were fixed with 4 % formaldehyde in phosphate-buffered saline (PBS) for 20 min at room temperature (RT). Cells were permeabilized with 0.3 % Triton X-100 in PBS for 30 min and blocked with 10 % normal goat serum (NGS) in 0.3 % Triton X-100 for 2 h at RT, followed by incubation with rabbit anti-PUMA (1:250; Cell Signaling, Danvers, MA, USA) at 4 ℃ overnight. The cells were then incubated with an AlexaFluor 488-conjuated anti-rabbit IgG secondary antibody (1:250; Invitrogen/Life Technologies, Grand Island, NY, USA) and mounted onto slides with mounting medium (Prolong Gold Anti-fade Reagent; Invitrogen/Life Technologies, Grand Island, NY, USA). PUMA expression was examined using an Olympus FV 1000 microscope, and quantification of fluorescence intensity was performed using ImageJ software.

Wounding-healing assay

A 600 µl volume of cell suspension containing C3H/10T1/2 cells (5x10^4 cells/ml) or HBVPs (5x10^4 cells/ml) was plated to form a monolayer. A cell-free straight line was created in the center of the well by scratching with a sterile 10-µl pipette tip. Similarly, a second straight line was scratched perpendicular to the first line to create a cross-shaped cellular gap in each well. Cell migration was quantified via florescence microscopy at 6 h or 12 h after methamphetamine treatment. Digital images (constant dimensions of 1000 × 800 µm) were captured using an EVOS® FL Cell Imaging microscope

(Invitrogen/Life Technologies, Grand Island, NY, USA) for 3–5 randomly selected microscopic fields in the wound. The maximum migration distance was determined by identifying the cell that had migrated the longest distance using ImageJ software.

Pericyte migration

Migration of pericyte *in vitro* was determined using a Boyden chamber (Corning Costar; Corning, Inc.,Corning, NY, USA) as described previously [27]. Cells was washed with PBS, then fluorescently labeled with 10 μM cell tracker green (Invitrogen) at 37 °C for 15 min. Labeled C3H/10T1/2 cells and HBVPs (1x10^6 cells) were added to the upper compartment of transwell inserts in serum-free medium and treated with methamphetamine. The transwell plates were incubated for 12 h at 37 °C, followed by quantification of pericyte migration by measuring the number of migrated cells following detachment of cells from the insert using a Synergy Mx fluorescent plate reader (BioTek Instruments, Winooski, VT, USA).

Pericyte adhesion assay

96-well plates were coated with 50 μl of fibronectin (Millipore) diluted with PBS (10 μg/ml) and were incubated for 1 h at 37 °C. BSA (1 % in PBS; 150 μl) was added to each well for 30 min at room temperature after removing the coated solution to block any remaining protein binding sites on the plates.

Then plates were washed with 150 µl of PBS for 3 times. Pericyte (2 x10^4 cells) labeled with 10 µM cell tracker green (Invitrogen) at 37 °C for 15 min were suspended in 200 µl of EMEM, followed by methamphetamine treatment. Pericyte were then washed 3 times with PBS to eliminate the nonadherent cells. Fluorescence intensity of adherent pericyte was measured using a Synergy Mx fluorescent plate reader (BioTek Instruments).

Lentiviral transduction of pericytes

Lentivirus containing green fluorescent protein (LV-GFP)-expressing shRNAs were purchased from Hanbio Inc. (Shanghai, China). Dissociated C3H/10T1/2 cells (5x10^4 cell/well) or HBVPs (5x10^4 cell/well) resuspended in 500 µl serum-free medium containing 8 µg/ml polybrene and 5 µl LV solution (10^8 IU/ml) were seeded in a 24-well plate. The suspensions were then gently swirled, and the plate was incubated at 37 °C and 5 % CO_2 for 24 h. Subsequently, the medium was replaced with 1 ml fresh medium containing 10 % FBS. Infected cells were placed in puromycin (1 µg/ml) to eliminate uninfected cells when the cell confluence reached 50%. Pure transduced pericyte cultures were expanded for further experiments.

Western blotting (WB)

Methamphetamine-treated cells were lysed using a Mammalian Cell Lysis Kit (Sigma-Aldrich, St. Louis, MO, USA). Protein concentrations were

determined using a BCA Protein Assay Kit (Beyotime Biotechnology, China). Then, equal amounts of proteins were subjected to 12% sodium dodecyl sulfate-polyacrylamide gel electrophoresis (SDS-PAGE) and transferred onto polyvinylidene fluoride (PVDF) membranes (Millipore, Billerica, MA, USA). The membranes were blocked with 5% non-fat dry milk in Tris-buffered saline with Tween-20 (TBST). The western blots were then probed with antibodies against PUMA, P-Erk/T-Erk, P-JNK/T-JNK, P-p38/T-p38, P-Akt/T-Akt, P-Src/T-Src, P-Pyk2/T-Pyk2, Bax, Bcl-xl, integrin β1, integrin β3 and GAPDH, purchased from Cell Signaling (Danvers, MA, USA; 1:1000), and an antibody against β-actin, obtained from Sigma-Aldrich (St. Louis, MO, USA; 1:1000). The secondary antibody used was horseradish peroxidase-conjugated to goat anti-mouse/rabbit IgG (1:2,000). Signals were detected by chemiluminescence and imaged using a Microchemi 4.2® (DNR, Israel) digital image scanner. Quantification was performed by densitometry using ImageJ software (NIH).

Statistical analysis

Statistical analysis was performed using GraphPad Prism V5 (Sorrento Valley, CA). Data are presented as the mean ± SEM. The significance of differences between the control and samples treated with the various drugs was determined by Student's t-test or one-way analysis of variance. A $p < 0.05$ was considered statistically significant.

Results

Methamphetamine-mediated up-regulation of PUMA in C3H/10T1/2 cells and HBVPs

Methamphetamine is known to be involved in the breakdown of BBB integrity, and recent studies have shown that pericyte dysfunction negatively affects the BBB integrity and structure [28, 29]. However, little is known about the influence of methamphetamine in pericytes; thus, we examined the detailed mechanisms underlying its effects. Our previous study has indicated that methamphetamine induces a transient increase in PUMA expression. Therefore, we sought to examine the role of PUMA in pericyte migration. To assess the effect of methamphetamine on expression of PUMA in pericytes, a pericyte-like cell line (C3H/10T1/2) and HBVPs were exposed to different concentrations of methamphetamine (10 μM, 100 μM, and 1mM) for 6 h and assessed for the expression of PUMA. As shown in Figure 1a and b, methamphetamine induced the expression of PUMA with peak response at a concentration of 100 μM. Thus, C3H/10T1/2 was treated with methamphetamine (100 μM) for various durations (15 min, 30 min, 1 h, 3 h, 6 h, 12 h, and 24 h), followed by protein extraction and measurement of PUMA expression. As shown in Figure 1c, PUMA expression was induced by methamphetamine as early as 30 min, and it continued to increase up 6 h in C3H/10T1/2 cells. These findings were further confirmed in primary HBVPs. As shown in Figure 1d, treatment of HBVPs with methamphetamine resulted in

increased PUMA expression in HBVPs, with peak expression detected at 3 h. These results were further confirmed by the immunostaining of cells treated with or without methamphetamine. As shown in Figure 1e and f, methamphetamine treatment increased PUMA expression in both C3H/10T1/2 cells and HBVPs. Taken together; these findings indicated that methamphetamine treatment increased expression of the PUMA protein in pericytes.

Involvement of PUMA in methamphetamine-mediated pericyte migration

Having determined that methamphetamine increases PUMA expression, we next examined the role of PUMA in pericyte migration. First, the effect of methamphetamine on pericyte migration was assessed. As shown in Figure 2a, methamphetamine treatment significantly induced the migration of C3H/10T1/2 cells, as determined by wounding-healing assay. Moreover, methamphetamine-induced migration dependent on its concentration and methamphetamine promoted significant migration with maximal response at a concentration of 100 μM (Supplementary Fig. 1a-b). Migration of C3H/10T1/2 in response to methamphetamine was also validated using the Boyden chambers (Fig 2c). Next, to examine the role of PUMA in pericyte migration, pericytes were transduced with a PUMA siRNA lentivirus. Knockdown of PUMA expression significantly decreased the methamphetamine-induced pericyte migration in C3H/10T1/2 cells (Fig. 2b-c). Cell migration is a multistep

biological process. To achieve migration, cells are required to assemble new focal adhesion at the migrating fronts and degrade extracellular matrix at the tailing edges [27, 30]. To explore the role of PUMA in pericyte adhesion, C3H/10T1/2 cells transduced with a PUMA siRNA lentivirus demonstrated significantly inhibition of adhesion (Fig 2d). Notably, knockdown of PUMA expression did not have any negative effects on C3H/10T1/2 cell viability, as shown in Figure 2e. The role of PUMA in pericyte migration and adhesion were further confirmed in primary HBVPs, as demonstrated by the finding that knockdown of PUMA expression significantly inhibited their migration and adhesion (Fig.2f-i). Consistent with its effects on the viability of C3H/10T1/2 cell, knockdown of PUMA expression did not negatively affect HBVP viability (Fig. 2j). As expected, transduction of cells with PUMA siRNA significantly decreased PUMA expression in both C3H/10T1/2 cells (Fig. 2k) and HBVPs (Fig. 2l). Therefore, these results have demonstrated that PUMA is involved in pericyte migration.

Methamphetamine-mediated up-regulation of PUMA involves activation of MAPK and PI3K/Akt pathways

Having determined that methamphetamine induces an increase in PUMA expression and plays a role in pericyte migration, we aimed to examine the potential signaling pathways involved in this process. Thus, we assessed the phosphorylation of MAPKs and PI3K/Akt in C3H/10T1/2 cells within 3 h of

exposure to methamphetamine. Treatment of cells with methamphetamine resulted in a time-dependent increase in the phosphorylation of ERK (Fig. 3a, upper panel), p38 (Fig. 3b, upper panel), JNK (Fig. 3c, upper panel), and Akt (Fig. 3d, upper panel), with activation occurring as early as 15 min. Because methamphetamine is known to bind to its cognate receptor, sigma-1 receptor, to exert its effects, we next examined the role of sigma-1 receptor in the activation of cell signaling pathways. Pre-treatment of pericytes with a sigma-1R antagonist, BD1047, significantly inhibited the methamphetamine-mediated activation of ERK (Fig. 3a, lower panel), p38 (Fig. 3b, lower panel), JNK (Fig. 3c, lower panel), and Akt (Fig. 3d, lower panel).

We next examined the roles of the MAPK and PI3K/Akt signaling pathways in the regulation of PUMA expression. C3H/10T1/2 cells were pretreated with an MEK1/2 inhibitor (U0126, 10 μM), p38 inhibitor (SB203580, 10 μM), JNK inhibitor (SP600125, 10 μM), or Akt inhibitor (LY294002, 5 μM) for 1 h, followed by treatment with methamphetamine for another 3 h. As shown in Figure 4a, pretreatment of cells with the MEK1/2 inhibitor, p38 inhibitor, JNK inhibitor, or Akt inhibitor significantly attenuated the increased PUMA expression induced by methamphetamine. These findings were further confirmed in primary HBVPs, as evidenced by the finding that these inhibitors significantly decreased the PUMA expression induced by methamphetamine (Fig. 4b). These results have indicated that methamphetamine-induced PUMA expression is mediated by MAPKs and the PI3K/Akt pathway.

Involvement of integrin β1 and β3 in methamphetamine-mediated pericyte migration

Integrins are cell surface adhesion molecules that act as bridges for cell-extracellular matrix connections, and they play key roles in tumor cell adhesion, migration and invasion [31, 32]. Thus, the next step was to elucidate whether integrins are involved in methamphetamine-induced pericyte migration. C3H/10T1/2 cells and HBVPs were treated with methamphetamine for varying durations (5 min to 3 h), and then integrin β1 and β3 levels were determined in cell lysates. We observed time-dependent alterations in the levels of integrin β1 and β3, which peaked at 6 h after treatment in both cell types (Fig. 5a and b). Next, to further identify the integrin subtypes participating in cell migration, we examined the effects of the functional blocking of integrin subtypes using neutralizing antibodies. Pretreatment of primary HBVPs with either neutralizing anti-β1 integrin or anti-β3 integrin resulted in the significant suppression of methamphetamine-mediated migration. However, treatment with the normal IgG antibody had no effect on pericyte migration (Fig. 5c). We next examined whether PUMA is critical for the activation of integrin signaling pathways. As shown in Figure 6a and b, knockdown of PUMA expression resulted in significant inhibition of the methamphetamine-induced expression of integrin β1 and β3 in primary HBVPs. These results thus underscore the roles of integrin β1 and β3 in the

methamphetamine-mediated induction of pericyte migration.

Involvement of tyrosine kinases Src and Pyk2 in methamphetamine-mediated pericyte migration

Having determined that integrin β1 and β3 are involved in pericyte migration, we next examined the molecules acting downstream of integrins. Our previous study has demonstrated that β1 and β3 integrin-cytoskeleton interactions are involved in Pyk2 and Src activation [27]. These proteins can be activated by integrin engagement with extracellular matrix proteins, resulting in their phosphorylation[33]. As shown in Figure 7a and c, Pyk2 and Src were phosphorylated at 15 min or 30 min after methamphetamine treatment, respectively. We next examined whether PUMA is critical for the activation of tyrosine kinase signaling pathways. As shown in Figure 7b and d, knockdown of PUMA expression also decreased the phosphorylation of Src and Pyk2. Collectively, these findings underscore the role of PUMA in the methamphetamine-mediated activation of downstream tyrosine kinase pathways.

Discussion

PUMA is a member of the BH3-only subgroup of the Bcl-2 family. It is a critical mediator of p53-dependent and p53-independent apoptosis and exerts strong pro-apoptotic effects. However, methamphetamine (100 μM) did not

significantly affect the level of Bax/Bcl-xl of C3H/10T1/2 cells or HBVPs (Supplementary Fig. 2a-b). The present study demonstrated that 1) methamphetamine treatment induced pericyte migration *in vitro* and that 2) PUMA promoted pericyte migration. Up-regulation of PUMA in pericytes may contribute to their migration through activation of integrin and tyrosine kinase mechanisms, thereby enhancing methamphetamine-induced BBB damage. Although our previous study has demonstrated that PUMA is involved in fibroblast migration, it remains unclear whether it plays a role in pericyte migration or contributes to methamphetamine-induced BBB damage[34].

Pericytes are located in microvascular walls and constitute the BBB, together with endothelial and astrocyte foot processes. These cells were first reported to function as mechanical components of microvessel walls. Disruption of BBB integrity occurs due to pericyte migration from microvascular walls, as evidenced by the finding of a separation between pericytes and the basement membrane, which was considered to reflect this migration[35]. In this study, we demonstrated that methamphetamine exposure induced a transient increase in PUMA expression in pericytes via a methamphetamine cognate receptor, sigma-1 receptor, which interacted with the MAPK and PI3K/Akt pathways, leading to PUMA expression with subsequent functional migration of pericytes. To the best of our knowledge, these results provide the first evidence of the critical role of PUMA in methamphetamine-mediated pericyte migration. Thus, these findings imply that PUMA is a promising

therapeutic target for amelioration of methamphetamine-mediated BBB damage via the targeting of pericytes.

Additionally, our study is the first to demonstrate that methamphetamine induces PUMA expression in pericytes via sigma-1 receptor, as pretreatment of cells with the sigma-1 receptor antagonist BD1047 or knockdown of sigma-1 receptor abrogated the increased PUMA expression induced by methamphetamine. We also examined the signaling pathways involved in methamphetamine-mediated PUMA up-regulation. Our previous studies have indicated that methamphetamine promotes MAPK and PI3K/Akt phosphorylation[36]. Using a pharmacological approach, our findings demonstrated that both the MAPK and PI3K/Akt pathways are involved in the methamphetamine-induced increase in PUMA expression, consistent with our previous study showing that these pathways are involved in SiO_2-induced PUMA expression in pulmonary fibroblasts[37]. Our findings are also consistent with a previous report showing that inhibition of the ERK pathway with U0126 significantly inhibits PUMA expression in melanoma [38].

Integrins belong to a family of cell adhesion molecules composed of 18 α and 8 β subunits that combine to form at least 24 heterodimers. β integrin associates with α subunits to form one of the largest subfamilies of integrin receptors that bind to a wide array of extracellular matrix molecules, including collagens, laminin and fibronectin[39]. Tiggers (2013) *et al* has demonstrated that under normal conditions, brain pericytes possess a high α5 integrin level

and low α1, α2, and α6 integrin levels. This expression pattern has a crucial role in the attachment of pericytes to vessel walls; in fact, an *in vivo* study has shown that TNF-α promotes pericyte proliferation and detachment, as well a switch in the integrin expression pattern with predominance of α2 integrin. Interestingly, α2 integrin expression has also been reported to be strongly correlated with brain vessel remodeling in experimental autoimmune encephalomyelitis[40]. Similarly, in Alzheimer's disease, fibrin deposition and increased extravascular IgG have been demonstrated to be correlated with reduced in pericyte coverage of endothelial cells[41] . Conditional deletion of β1 integrin in endothelial cells results in abnormal vascular development and lethality during the embryonic period [42]. A previous study has indicated that the NG2 proteoglycan facilitates the proliferation and motility of human brain pericytes via activation of β1 integrin, as evidenced by the finding that knockdown of NG2 expression results in diminished activation of β1 integrin signaling in NG2-deficient pericytes[43]. Our current findings have demonstrated the role of PUMA in methamphetamine–induced pericyte migration and have indicated that integrin β1 and β3, acting downstream of PUMA, are key targets for the regulation of pericyte migration. These findings are consistent with those of a previous study showing that the expression of both integrin β1 and β3 in pericytes regulates postangiogenic neovessel survival in collagen and fibrin matrices [44]. In addition, methamphetamine has been reported to regulate the expression of integrin family members that are

involved in intracellular signaling cascades, thereby affecting cell survival[45]. Further, our previous study has demonstrated that integrin β1, but not β3, is involved in the microglial migration induced by the HIV Tat protein [27]. However, in the current study, both β1 and β3 integrins were involved in pericyte migration. These discrepant findings among studies may be due to differences in the cell systems examined.

The binding of ligands, such as HIV Tat, to α5β1 and αvβ3 integrins via its RGD-rich domain regulates endothelial cell cycle progression [46, 47]. In contrast, our studies of the effects of methamphetamine treatment on β1 and β3 integrins, which lack RGD domains, have demonstrated their “inside-out” activation. This leads to an “outside-in” signal that results in activation of the Src and Pyk2 kinases, resulting in actin polymerization, thereby reinforcing the integrin-cytoskeleton interactions and keeping β1 and β3 integrins in high-affinity and high-avidity states, reflecting their full activation[48]. Integrin-matrix interactions, in turn, induce "outside-in" signals to activate the tyrosine kinases Src and Pyk2 [49, 50]. In the current study, knockdown of PUMA expression significantly inhibited integrin β1 and β3 expression, as well as tyrosine kinase phosphorylation, suggesting that PUMA acts upstream of these signaling pathways. Moreover, although the present study revealed the detailed underlying mechanisms by which methamphetamine increases PUMA expression, the precise mechanism by which PUMA promotes migration needs to be elucidated.

Pericyte loss/dysfunction or their diminished attachment to endothelial cells is known to be associated with an increased number of "leaky" microvessels in multiple sclerosis (MS), Alzheimer's disease, amyotrophic lateral sclerosis (ALS), and stroke as contributors to BBB impairment, neuroinflammation, and neuronal demise. We hypothesized that pericyte dysfunction is involved in methamphetamine-mediated BBB impairment. We showed that pericyte coverage was markedly decreased in the brains of HIV-infected patients. We profiled the phenotypic changes that occurred during exposure to HIV/relevant inflammatory factors and examined their correlations with functional stability of the BBB *in vitro* and with pericyte secretion of molecules supporting barrier function. Our data indicated that under inflammatory conditions, pericytes switched to a pro-inflammatory phenotype and produced inflammatory factors associated with HIV-1 neuroinflammation. The limitation of our current study was that we could not provide evidence that amelioration of pericyte coverage blocked the methamphetamine-induced BBB damage in PUMA knockdown cells. In our on-going study, PUMA knockdown was found to decrease TJP expression, whereas it was increased by PUMA overexpression. These findings, along with those of a previous report showing that the number of endothelial cells in the retina in PUMA knockout mice is significantly decreased compared with that in wild-type mice[24], suggest a novel function of PUMA in BBB integrity. Distinct roles of PUMA in different cellular environments could provide an explanation for this inconsistency.

Therefore, elucidating the distinct roles of PUMA in different cell types could help to increase the current understanding of the detailed mechanisms underlying its diverse functions in different contexts. Experiments using pericytes with the conditional knockout of PUMA will be worth conducting in future investigations.

Conclusions

In summary, our findings have revealed the detailed molecular mechanisms involved in the methamphetamine-mediated migration of pericytes via sigma-1 receptor, with downstream activation of the MAPK and PI3K/Akt pathways, resulting in increased PUMA expression. These findings have implications for understanding methamphetamine-induced pericyte migration. The targeting of PUMA can be considered a therapeutic strategy for the treatment of methamphetamine-induced BBB damage.

Acknowledgements

This work was supported by grants from the National Natural Science Foundation of China (No. 81322048 and No. 81473190). We were also awarded grants from the Jiangsu Specially Appointed Professor and the Major State Basic Research Development Program of China (973 Program) (2013CB733800, 2013CB733803) and the Postdoctoral Research Start Foundation of Southeast University (1124000342).

Author contributions

Y.H. planned and designed the research, supervised the experiments and wrote the manuscript; Y.H.Z carried out the cell cultures, performed the immunostaining and western blotting; Y.Z. carried out the migration assay, analyzed the data and generated the figures; Y.B. participated in data acquisition and analysis; J.C participated in the design of study, drafted manuscript and coordinated the lab work; and G.H. provided the comments on the manuscript, edited the writing, and involved in revising it critically for important intellectual content. All authors read and approved the final manuscript.

Competing interests

The authors declare no competing financial interests.

References

[1] Persidsky, Y., S.H. Ramirez, J. Haorah, and G.D. Kanmogne, *Blood-brain barrier: structural components and function under physiologic and pathologic conditions.* J Neuroimmune Pharmacol, 2006. **1**(3): p. 223-36.

[2] Argaw, A.T., L. Asp, J. Zhang, K. Navrazhina, T. Pham, J.N. Mariani, S. Mahase, D.J. Dutta, J. Seto, E.G. Kramer, N. Ferrara, M.V. Sofroniew,

and G.R. John, *Astrocyte-derived VEGF-A drives blood-brain barrier disruption in CNS inflammatory disease.* J Clin Invest, 2012. **122**(7): p. 2454-68.

[3] Abbott, N.J., L. Ronnback, and E. Hansson, *Astrocyte-endothelial interactions at the blood-brain barrier.* Nat Rev Neurosci, 2006. **7**(1): p. 41-53.

[4] Yao, Y., Z.L. Chen, E.H. Norris, and S. Strickland, *Astrocytic laminin regulates pericyte differentiation and maintains blood brain barrier integrity.* Nat Commun, 2014. **5**: p. 3413.

[5] van Vliet, E.A., S. da Costa Araujo, S. Redeker, R. van Schaik, E. Aronica, and J.A. Gorter, *Blood-brain barrier leakage may lead to progression of temporal lobe epilepsy.* Brain, 2007. **130**(Pt 2): p. 521-34.

[6] Zipser, B.D., C.E. Johanson, L. Gonzalez, T.M. Berzin, R. Tavares, C.M. Hulette, M.P. Vitek, V. Hovanesian, and E.G. Stopa, *Microvascular injury and blood-brain barrier leakage in Alzheimer's disease.* Neurobiol Aging, 2007. **28**(7): p. 977-86.

[7] Wardlaw, J.M., F. Doubal, P. Armitage, F. Chappell, T. Carpenter, S. Munoz Maniega, A. Farrall, C. Sudlow, M. Dennis, and B. Dhillon, *Lacunar stroke is associated with diffuse blood-brain barrier dysfunction.* Ann Neurol, 2009. **65**(2): p. 194-202.

[8] Kaushal, N. and R.R. Matsumoto, *Role of sigma receptors in*

methamphetamine-induced neurotoxicity. Curr Neuropharmacol, 2011. **9**(1): p. 54-7.

[9] Schepers, R.J., J.M. Oyler, R.E. Joseph, Jr., E.J. Cone, E.T. Moolchan, and M.A. Huestis, *Methamphetamine and amphetamine pharmacokinetics in oral fluid and plasma after controlled oral methamphetamine administration to human volunteers.* Clin Chem, 2003. **49**(1): p. 121-32.

[10] Urrutia, A., A. Rubio-Araiz, M.D. Gutierrez-Lopez, A. ElAli, D.M. Hermann, E. O'Shea, and M.I. Colado, *A study on the effect of JNK inhibitor, SP600125, on the disruption of blood-brain barrier induced by methamphetamine.* Neurobiol Dis, 2013. **50**: p. 49-58.

[11] Martins, T., T. Burgoyne, B.A. Kenny, N. Hudson, C.E. Futter, A.F. Ambrosio, A.P. Silva, J. Greenwood, and P. Turowski, *Methamphetamine-induced nitric oxide promotes vesicular transport in blood-brain barrier endothelial cells.* Neuropharmacology, 2013. **65**: p. 74-82.

[12] Bowyer, J.F. and S. Ali, *High doses of methamphetamine that cause disruption of the blood-brain barrier in limbic regions produce extensive neuronal degeneration in mouse hippocampus.* Synapse, 2006. **60**(7): p. 521-32.

[13] Sharma, H.S. and E.A. Kiyatkin, *Rapid morphological brain abnormalities during acute methamphetamine intoxication in the rat: an*

experimental study using light and electron microscopy. J Chem Neuroanat, 2009. **37**(1): p. 18-32.

[14] Melgar, M.A., J. Rafols, D. Gloss, and F.G. Diaz, *Postischemic reperfusion: ultrastructural blood-brain barrier and hemodynamic correlative changes in an awake model of transient forebrain ischemia.* Neurosurgery, 2005. **56**(3): p. 571-81.

[15] Parikh, N.U., R. Aalinkeel, J.L. Reynolds, B.B. Nair, D.E. Sykes, M.J. Mammen, S.A. Schwartz, and S.D. Mahajan, *Galectin-1 suppresses methamphetamine induced neuroinflammation in human brain microvascular endothelial cells: Neuroprotective role in maintaining blood brain barrier integrity.* Brain Res, 2015. **1624**: p. 175-87.

[16] Cai, D., E. Huang, B. Luo, Y. Yang, F. Zhang, C. Liu, Z. Lin, W.B. Xie, and H. Wang, *Nupr1/Chop signal axis is involved in mitochondrion-related endothelial cell apoptosis induced by methamphetamine.* Cell Death Dis, 2016. **7**: p. e2161.

[17] Bowyer, J.F., S. Sarkar, K.M. Tranter, J.P. Hanig, D.B. Miller, and J.P. O'Callaghan, *Vascular-directed responses of microglia produced by methamphetamine exposure: indirect evidence that microglia are involved in vascular repair?* J Neuroinflammation, 2016. **13**(1): p. 64.

[18] Hill, J., S. Rom, S.H. Ramirez, and Y. Persidsky, *Emerging roles of pericytes in the regulation of the neurovascular unit in health and disease.* J Neuroimmune Pharmacol, 2014. **9**(5): p. 591-605.

[19] Daneman, R., L. Zhou, A.A. Kebede, and B.A. Barres, *Pericytes are required for blood-brain barrier integrity during embryogenesis.* Nature, 2010. **468**(7323): p. 562-6.

[20] Dore-Duffy, P., *Pericytes: pluripotent cells of the blood brain barrier.* Curr Pharm Des, 2008. **14**(16): p. 1581-93.

[21] Dore-Duffy, P. and K. Cleary, *Morphology and properties of pericytes.* Methods Mol Biol, 2011. **686**: p. 49-68.

[22] Vavrova, J. and M. Rezacova, *Importance of proapoptotic protein PUMA in cell radioresistance.* Folia Biol (Praha), 2014. **60**(2): p. 53-6.

[23] Hikisz, P. and Z.M. Kilianska, *PUMA, a critical mediator of cell death--one decade on from its discovery.* Cell Mol Biol Lett, 2012. **17**(4): p. 646-69.

[24] Zhang, F., Y. Li, Z. Tang, A. Kumar, C. Lee, L. Zhang, C. Zhu, A. Klotzsche-von Ameln, B. Wang, Z. Gao, S. Zhang, H.F. Langer, X. Hou, L. Jensen, W. Ma, W. Wong, T. Chavakis, Y. Liu, Y. Cao, and X. Li, *Proliferative and survival effects of PUMA promote angiogenesis.* Cell Rep, 2012. **2**(5): p. 1272-85.

[25] Bai, Y., X. Zhu, J. Chao, Y. Zhang, C. Qian, P. Li, D. Liu, B. Han, L. Zhao, J. Zhang, S. Buch, G. Teng, G. Hu, and H. Yao, *Pericytes contribute to the disruption of the cerebral endothelial barrier via increasing VEGF expression: implications for stroke.* PLoS One, 2015. **10**(4): p. e0124362.

[26] Zhang, Y., T. Zhu, X. Zhang, J. Chao, G. Hu, and H. Yao, *Role of high-mobility group box 1 in methamphetamine-induced activation and migration of astrocytes.* J Neuroinflammation, 2015. **12**: p. 156.

[27] Yao, H., M. Duan, L. Yang, and S. Buch, *Nonmuscle myosin light-chain kinase mediates microglial migration induced by HIV Tat: involvement of beta1 integrins.* FASEB J, 2013. **27**(4): p. 1532-48.

[28] Armulik, A., G. Genove, M. Mae, M.H. Nisancioglu, E. Wallgard, C. Niaudet, L. He, J. Norlin, P. Lindblom, K. Strittmatter, B.R. Johansson, and C. Betsholtz, *Pericytes regulate the blood-brain barrier.* Nature, 2010. **468**(7323): p. 557-61.

[29] Bell, R.D., E.A. Winkler, A.P. Sagare, I. Singh, B. LaRue, R. Deane, and B.V. Zlokovic, *Pericytes control key neurovascular functions and neuronal phenotype in the adult brain and during brain aging.* Neuron, 2010. **68**(3): p. 409-27.

[30] Caswell, P.T., S. Vadrevu, and J.C. Norman, *Integrins: masters and slaves of endocytic transport.* Nat Rev Mol Cell Biol, 2009. **10**(12): p. 843-53.

[31] Kamranvar, S.A., D.K. Gupta, Y. Huang, R.K. Gupta, and S. Johansson, *Integrin signaling via FAK-Src controls cytokinetic abscission by decelerating PLK1 degradation and subsequent recruitment of CEP55 at the midbody.* Oncotarget, 2016.

[32] Seguin, L., J.S. Desgrosellier, S.M. Weis, and D.A. Cheresh, *Integrins*

and cancer: regulators of cancer stemness, metastasis, and drug resistance. Trends Cell Biol, 2015. **25**(4): p. 234-40.

[33] Miao, L., X. Xin, H. Xin, X. Shen, and Y.Z. Zhu, *Hydrogen Sulfide Recruits Macrophage Migration by Integrin beta1-Src-FAK/Pyk2-Rac Pathway in Myocardial Infarction.* Sci Rep, 2016. **6**: p. 22363.

[34] Hurtado-Alvarado, G., A.M. Cabanas-Morales, and B. Gomez-Gonzalez, *Pericytes: brain-immune interface modulators.* Front Integr Neurosci, 2014. **7**: p. 80.

[35] Duz, B., E. Oztas, T. Erginay, E. Erdogan, and E. Gonul, *The effect of moderate hypothermia in acute ischemic stroke on pericyte migration: an ultrastructural study.* Cryobiology, 2007. **55**(3): p. 279-84.

[36] Shen, K., Y. Zhang, X. Lv, X. Chen, R. Zhou, L.K. Nguyen, X. Wu, and H. Yao, *Molecular Mechanisms Involving Sigma-1 Receptor in Cell Apoptosis of BV-2 Microglial Cells Induced by Methamphetamine.* CNS Neurol Disord Drug Targets, 2016.

[37] Wang, W., H. Liu, X. Dai, S. Fang, X. Wang, Y. Zhang, H. Yao, X. Zhang, and J. Chao, *p53/PUMA expression in human pulmonary fibroblasts mediates cell activation and migration in silicosis.* Sci Rep, 2015. **5**: p. 16900.

[38] Haydn, J.M., A. Hufnagel, J. Grimm, K. Maurus, M. Schartl, and S. Meierjohann, *The MAPK pathway as an apoptosis enhancer in melanoma.* Oncotarget, 2014. **5**(13): p. 5040-53.

[39] Hynes, R.O., *Integrins: bidirectional, allosteric signaling machines.* Cell, 2002. **110**(6): p. 673-87.

[40] Tigges, U., A. Boroujerdi, J.V. Welser-Alves, and R. Milner, *TNF-alpha promotes cerebral pericyte remodeling in vitro, via a switch from alpha1 to alpha2 integrins.* J Neuroinflammation, 2013. **10**: p. 33.

[41] Sengillo, J.D., E.A. Winkler, C.T. Walker, J.S. Sullivan, M. Johnson, and B.V. Zlokovic, *Deficiency in mural vascular cells coincides with blood-brain barrier disruption in Alzheimer's disease.* Brain Pathol, 2013. **23**(3): p. 303-10.

[42] He, C., H. Hu, R. Braren, S.Y. Fong, A. Trumpp, T.R. Carlson, and R.A. Wang, *c-myc in the hematopoietic lineage is crucial for its angiogenic function in the mouse embryo.* Development, 2008. **135**(14): p. 2467-77.

[43] You, W.K., F. Yotsumoto, K. Sakimura, R.H. Adams, and W.B. Stallcup, *NG2 proteoglycan promotes tumor vascularization via integrin-dependent effects on pericyte function.* Angiogenesis, 2014. **17**(1): p. 61-76.

[44] Carnevale, E., E. Fogel, A.C. Aplin, M. Gelati, K.M. Howson, W.H. Zhu, and R.F. Nicosia, *Regulation of postangiogenic neovessel survival by beta1 and beta3 integrins in collagen and fibrin matrices.* J Vasc Res, 2007. **44**(1): p. 40-50.

[45] Betts, E.S., I.N. Krasnova, M.T. McCoy, B. Ladenheim, and J.L. Cadet,

Analysis of methamphetamine-induced changes in the expression of integrin family members in the cortex of wild-type and c-fos knockout mice. Neurotox Res, 2002. **4**(7-8): p. 617-623.

[46] Toschi, E., I. Bacigalupo, R. Strippoli, C. Chiozzini, A. Cereseto, M. Falchi, F. Nappi, C. Sgadari, G. Barillari, F. Mainiero, and B. Ensoli, *HIV-1 Tat regulates endothelial cell cycle progression via activation of the Ras/ERK MAPK signaling pathway.* Mol Biol Cell, 2006. **17**(4): p. 1985-94.

[47] Urbinati, C., S. Mitola, E. Tanghetti, C. Kumar, J. Waltenberger, D. Ribatti, M. Presta, and M. Rusnati, *Integrin alphavbeta3 as a target for blocking HIV-1 Tat-induced endothelial cell activation in vitro and angiogenesis in vivo.* Arterioscler Thromb Vasc Biol, 2005. **25**(11): p. 2315-20.

[48] Lu, L., C. Lin, Z. Yan, S. Wang, Y. Zhang, S. Wang, J. Wang, C. Liu, and J. Chen, *Kindlin-3 Is essential for the resting α4β1 integrin-mediated firm cell adhesion under shear flow conditions.* J Biol Chem, 2016. **291**(19): p. 10363-71.

[49] Calderwood, D.A., S.J. Shattil, and M.H. Ginsberg, *Integrins and actin filaments: reciprocal regulation of cell adhesion and signaling.* J Biol Chem, 2000. **275**(30): p. 22607-10.

[50] Totani, L., A. Piccoli, S. Manarini, L. Federico, R. Pecce, N. Martelli, C. Cerletti, P. Piccardoni, C.A. Lowell, S.S. Smyth, G. Berton, and V.

Evangelista, *Src-family kinases mediate an outside-in signal necessary for beta2 integrins to achieve full activation and sustain firm adhesion of polymorphonuclear leucocytes tethered on E-selectin.* Biochem J, 2006. **396**(1): p. 89-98.

Figure legends

Figure 1 Methamphetamine mediates PUMA up-regulation in both C3H/10T1/2 cells and HBVPs. (**a, b**) C3H/10T1/2 cells (**a**) and HBVPs (**b**) were incubated with varying concentrations of methamphetamine (10 μM, 100 μM, and 1mM) for 6 h. Representative immunoblots and the densitometric analysis of PUMA/GAPDH. **p* < 0.05 and ***p* < 0.01 versus the control group. n = 3. (**c, d**) Methamphetamine induced PUMA expression in a time-dependent manner in C3H/10T1/2 cells (**c**) and primary HBVPs (**d**). **p* < 0.05; ***p* < 0.01 and ****p* < 0.001 versus the control group using one-way ANOVA. n = 3. (**e, f**) Representative immunofluorescence staining for PUMA (green) in C3H/10T1/2 cells (**e**) and HBVPs (**f**) treated with methamphetamine (100 μM) for 30 min and 3 h, respectively. Green, PUMA; Blue, DAPI. Scale bars = 50 μm. Quantification of PUMA immunofluorescence intensity from five areas of the slides in C3H/10T1/2 cells and HBVPs using ImageJ software. IOD-integrated optical density. **p* < 0.05 and ****p* < 0.001 versus the control group using Student's t-test. All data are presented as the mean ± SEM of three individual experiments.

Figure 2 Involvement of PUMA in methamphetamine-mediated pericyte migration. (**a**) Representative images showing the migration of C3H/10T1/2 cells by wound-healing assay. (**b**) Quantification of the gap width was evaluated for C3H/10T1/2 cells using ImageJ software. (**c**) C3H/10T1/2 cells transduced with a PUMA siRNA lentivirus inhibited methamphetamine-induced

migration. (**d**) Knock down of PUMA inhibited methamphetamine-induced adhesion. (**e**) The viability of C3H/10T1/2 cells was determined by MTT assay. (**f**) Representative images showing the migration of HBVPs by wound-healing assay. (**g**) The gap width was quantitatively evaluated for HBVPs using ImageJ software. (**h**) HBVPs transduced with a PUMA siRNA lentivirus inhibited methamphetamine-induced migration. (**i**) Knock down of PUMA inhibited methamphetamine-induced adhesion. (**j**) The viability of HBVPs was determined by MTT assay. (**k**) C3H/10T1/2 cells were transduced with a PUMA siRNA lentivirus for 24 h, followed by treatment with methamphetamine (100 μM) for another 24 h. Then, the cells were processed for detection of PUMA expression by western blotting. (**l**) Transduction of HBVPs with a PUMA siRNA lentivirus successfully decreased PUMA expression. Scale bars = 400 μm. All data are presented as the mean ± SEM of three individual experiments. *p < 0.05; **p < 0.01 and ***p < 0.001 versus the control group at the corresponding time point. #p < 0.05 and ##p < 0.01 versus the methamphetamine-treated group using one-way ANOVA.

Figure 3 Methamphetamine mediates activation of MAPK and PI3K/Akt pathways. (**a**) Methamphetamine mediated activation of Erk (**a**, upper panel) in a time-dependent manner in C3H/10T1/2 cells, and pretreatment of C3H/10T1/2 cells with a sigma-1 receptor antagonist (BD 1047; 10 μM) resulted in inhibition of the methamphetamine-induced phosphorylation of Erk (**a**, lower panel). (**b**) Methamphetamine induced p38 phosphorylation (**b**, upper

panel), and pretreatment of C3H/10T1/2 cells with a sigma-1 receptor antagonist (BD 1047; 10 μM) inhibited the methamphetamine-induced phosphorylation of p38 (**b**, lower panel). (**c**) Methamphetamine mediated activation of JNK (C, upper panel), and pretreatment of C3H/10T1/2 cells with a sigma-1 receptor antagonist (BD 1047; 10 μM) inhibited the methamphetamine-induced phosphorylation of JNK (**c**, lower panel). (**d**) Methamphetamine mediated activation of PI3K/Akt (**d**, upper panel), and pretreatment of C3H/10T1/2 cells with a sigma-1 receptor antagonist (BD 1047; 10 μM) resulted in inhibition of the methamphetamine-induced phosphorylation of Akt (**d**, lower panel). All data are presented as the mean ± SEM of three individual experiments. *p < 0.05; **p < 0.01 and ***p < 0.001 versus the control group. #p < 0.05; ##p < 0.01 and ###p < 0.001 versus the methamphetamine-treated group using one-way ANOVA.

Figure 4 Methamphetamine-mediated induction of PUMA expression involves activation of MAPK and PI3K/Akt pathways. (**a, b**) Pharmacologic inhibition of the Erk, p38, JNK and Akt pathways with an MEK1/2 inhibitor (U0126, 10 μM), p38 inhibitor (SB203580, 10 μM), JNK inhibitor (SP600125, 10 μM) and PI3K inhibitor (LY294002, 5 μM) resulted in amelioration of the methamphetamine-mediated induction of PUMA expression in C3H/10T1/2 cells (**a**) and HBVPs (**b**). All data are presented as the mean ± SEM of three individual experiments. ***p < 0.001 versus the control group. #p < 0.05; ##p <

0.01 and ###p < 0.001 versus the methamphetamine-treated group using one-way ANOVA.

Figure 5 Involvement of integrin β1 and β3 in methamphetamine-induced pericyte migration. (**a, b**) Methamphetamine time-dependently increased integrin β1 and β3 protein expression in C3H/10T1/2 cells (**a**) and HBVPs (**b**). (**c**) HBVPs pretreated with a neutralizing integrin β1 or β3 antibody (1 μg/ml) were exposed to methamphetamine, and then cell migration assay was performed. Neutralizing integrin β1 or β3 significantly inhibited methamphetamine-induced pericyte migration, whereas IgG had no effect. Scale bars, 400 μm. All data are presented as the mean ± SEM of three individual experiments. *p < 0.05; **p < 0.01 and ***p < 0.001 versus the control group. #p < 0.05 and ##p < 0.01 versus the methamphetamine-treated group using one-way ANOVA.

Figure 6 Role of PUMA in methamphetamine-mediated integrin up-regulation. (**a, b**) Knockdown of PUMA expression resulted in inhibition of the methamphetamine-mediated increase in integrin β1 (**a**) and integrin β3 (**b**) expression in primary HBVPs. All data are presented as the mean ± SEM of three individual experiments. *p < 0.05 and ***p < 0.001 versus the control group. ##p < 0.01 versus the methamphetamine-treated group using one-way ANOVA.

Figure 7 Involvement of tyrosine kinases Src and Pyk2 in methamphetamine-mediated pericyte migration. (**a, b**) Western blotting

revealed the time-dependent activation of the tyrosine kinases Src and Pyk2 by methamphetamine in both C3H/10T1/2 cells (**a**) and primary HBVPs (**b**). (**c, d**) Knockdown of PUMA expression resulted in inhibition of the methamphetamine-mediated phosphorylation of Src (**c**) and Pyk2 (**d**). All data are presented as the mean ± SEM of three individual experiments. ***p < 0.001 versus the control group. ##p < 0.01 and ###p < 0.001 versus the methamphetamine-treated group using one-way ANOVA.

Highlights

Methamphetamine enhanced pericytes migration.

Knockdown of PUMA expression inhibited pericytes migration and adhesion.

Integrin β1 and β3 expression were involved in pericytes migration.

Fig 1

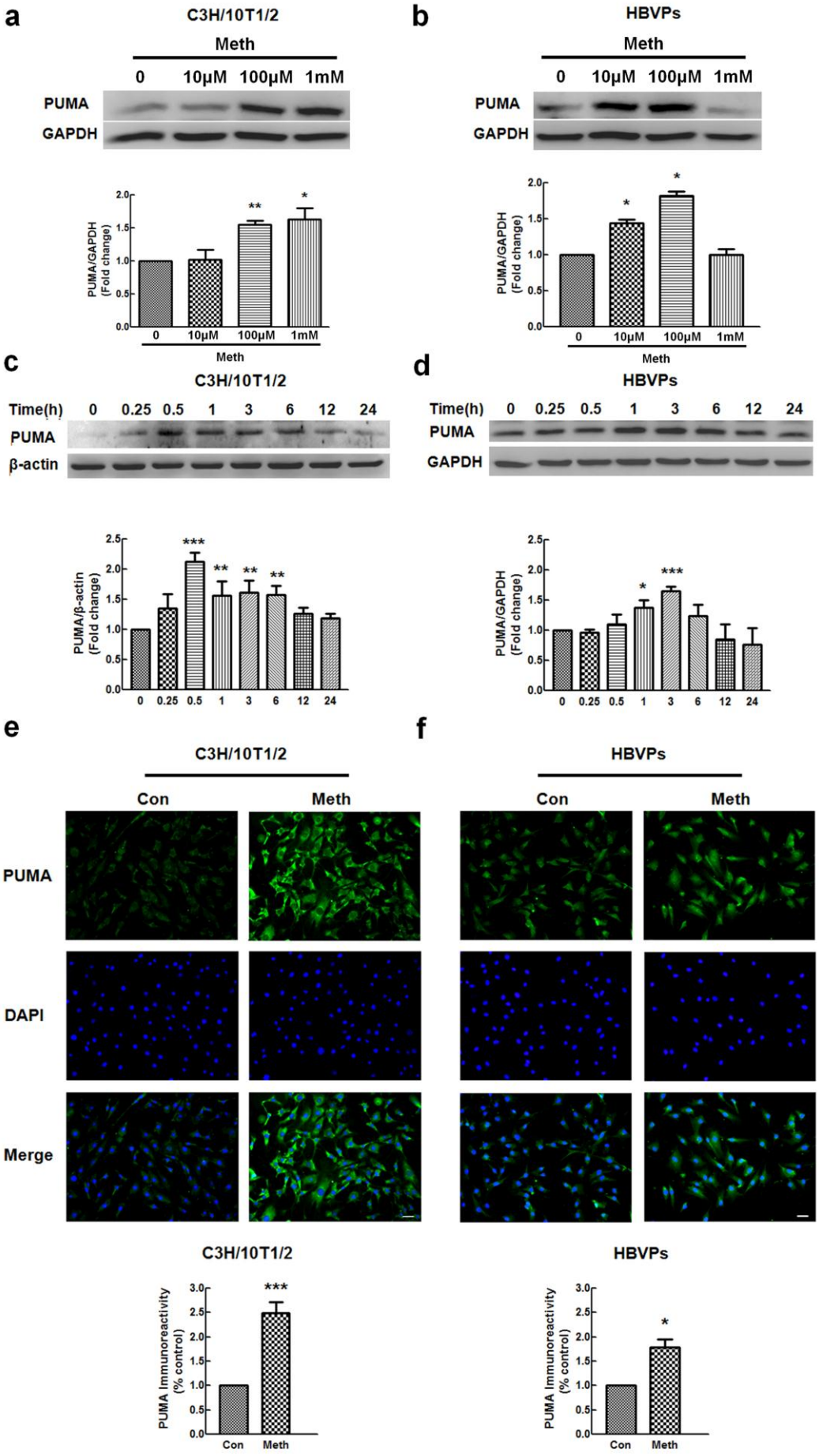
a
C3H/10T1/2
Meth
0 10μM 100μM 1mM
PUMA
GAPDH
PUMA/GAPDH (Fold change)
Meth
b
HBVPs
c
C3H/10T1/2
Time(h) 0 0.25 0.5 1 3 6 12 24
PUMA
β-actin
PUMA/β-actin (Fold change)
d
HBVPs
GAPDH
e
C3H/10T1/2
Con Meth
PUMA
DAPI
Merge
PUMA Immunoreactivity (% control)
f
HBVPs

Fig 2

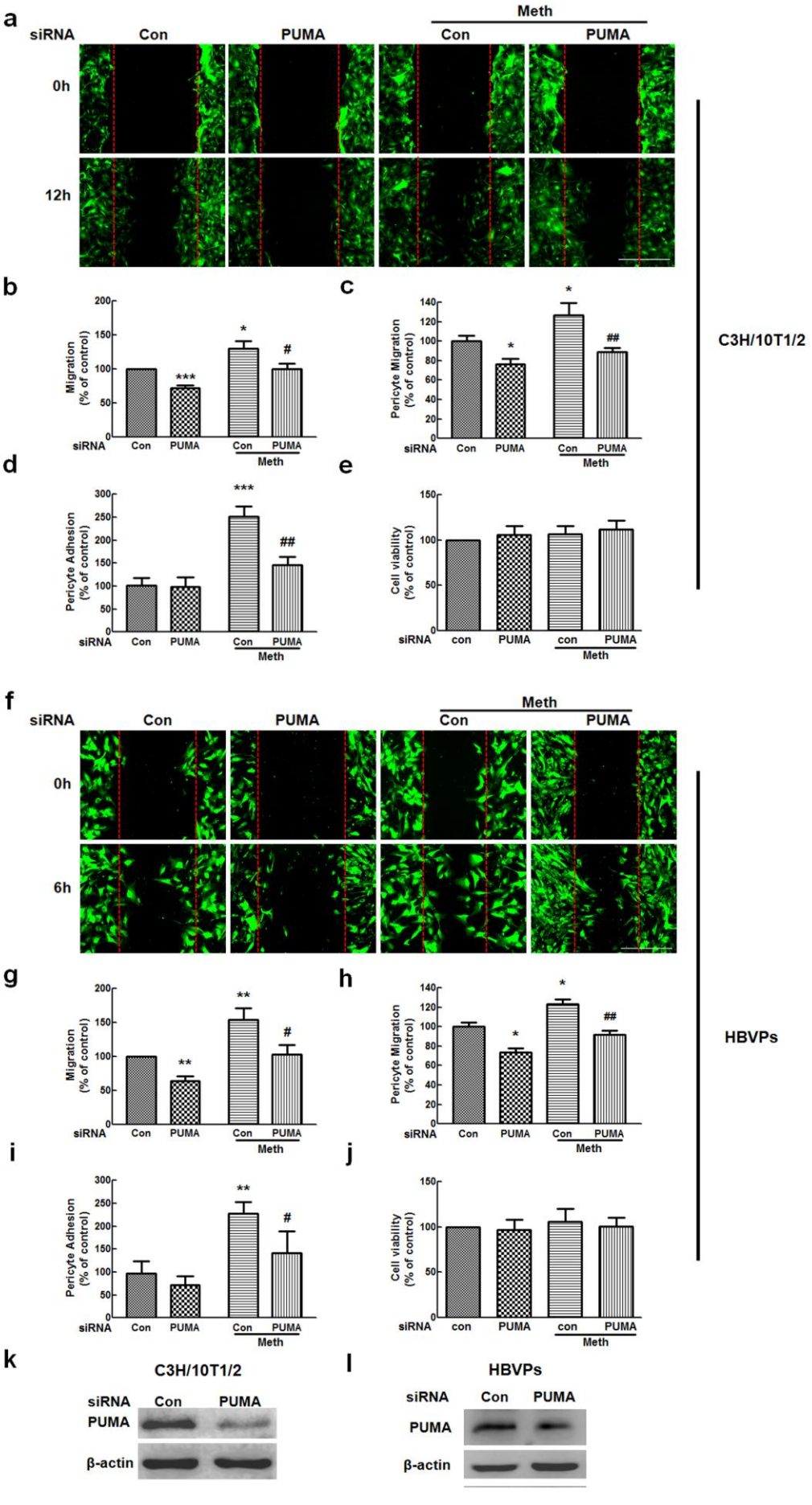
a
siRNA
Con
PUMA
Meth
Con
PUMA
0h
12h
b
Migration (% of control)
siRNA
Con
PUMA
Con
PUMA
Meth
c
Pericyte Migration (% of control)
d
Pericyte Adhesion (% of control)
e
Cell viability (% of control)
C3H/10T1/2
f
siRNA
Con
PUMA
Meth
Con
PUMA
0h
6h
g
Migration (% of control)
h
Pericyte Migration (% of control)
i
Pericyte Adhesion (% of control)
j
Cell viability (% of control)
HBVPs
k
C3H/10T1/2
siRNA
Con
PUMA
PUMA
β-actin
l
HBVPs
siRNA
Con
PUMA
PUMA
β-actin

Fig 3

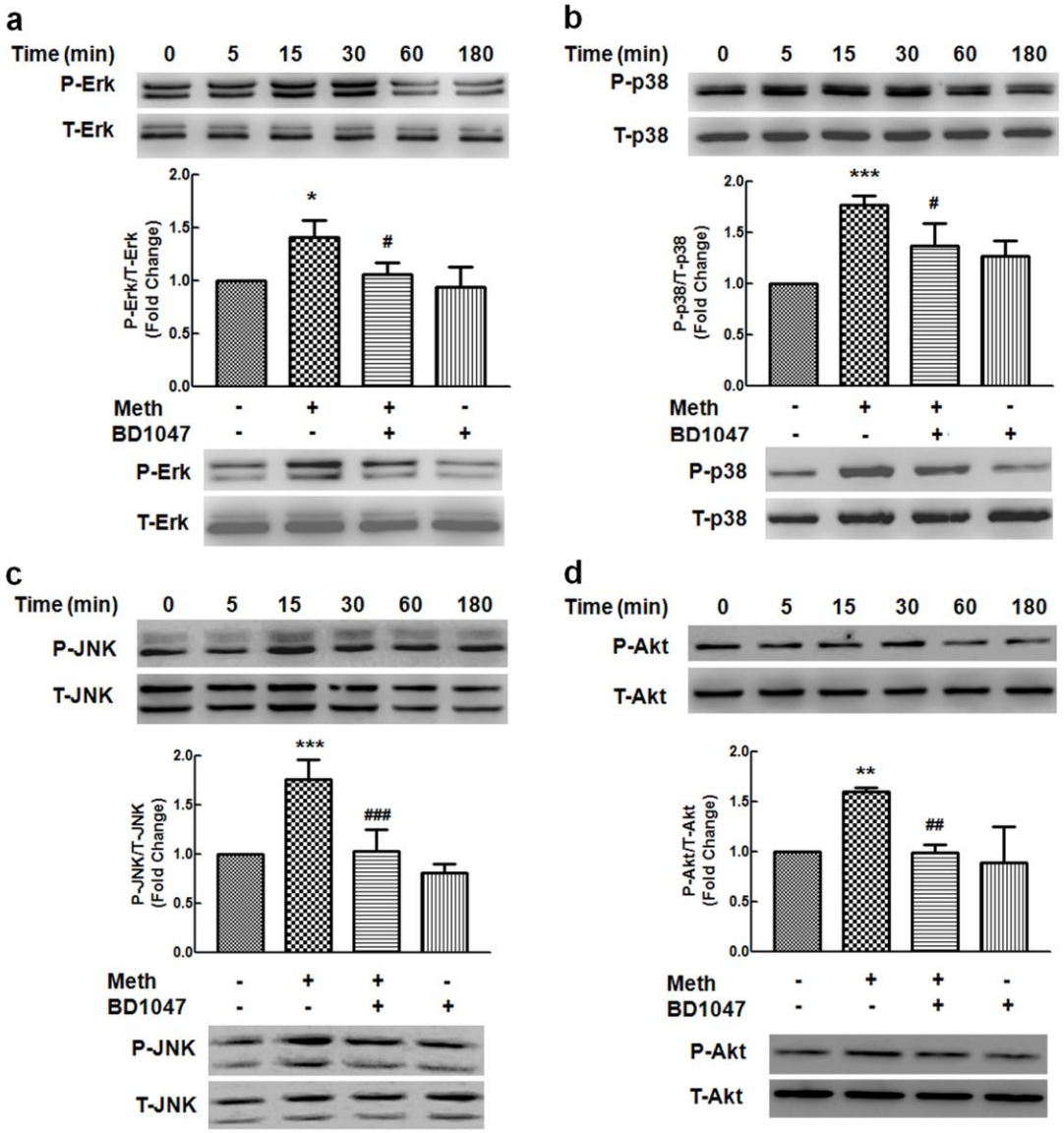
a
Time (min) 0 5 15 30 60 180
P-Erk
T-Erk
P-Erk/T-Erk (Fold Change)
2.0
1.5
1.0
0.5
0.0
*
#
Meth - + + -
BD1047 - - + +
P-Erk
T-Erk
b
Time (min) 0 5 15 30 60 180
P-p38
T-p38
P-p38/T-p38 (Fold Change)
***
#
Meth - + + -
BD1047 - - + +
P-p38
T-p38
c
Time (min) 0 5 15 30 60 180
P-JNK
T-JNK
P-JNK/T-JNK (Fold Change)
***
###
Meth - + + -
BD1047 - - + +
P-JNK
T-JNK
d
Time (min) 0 5 15 30 60 180
P-Akt
T-Akt
P-Akt/T-Akt (Fold Change)
**
##
Meth - + + -
BD1047 - - + +
P-Akt
T-Akt

Fig 4

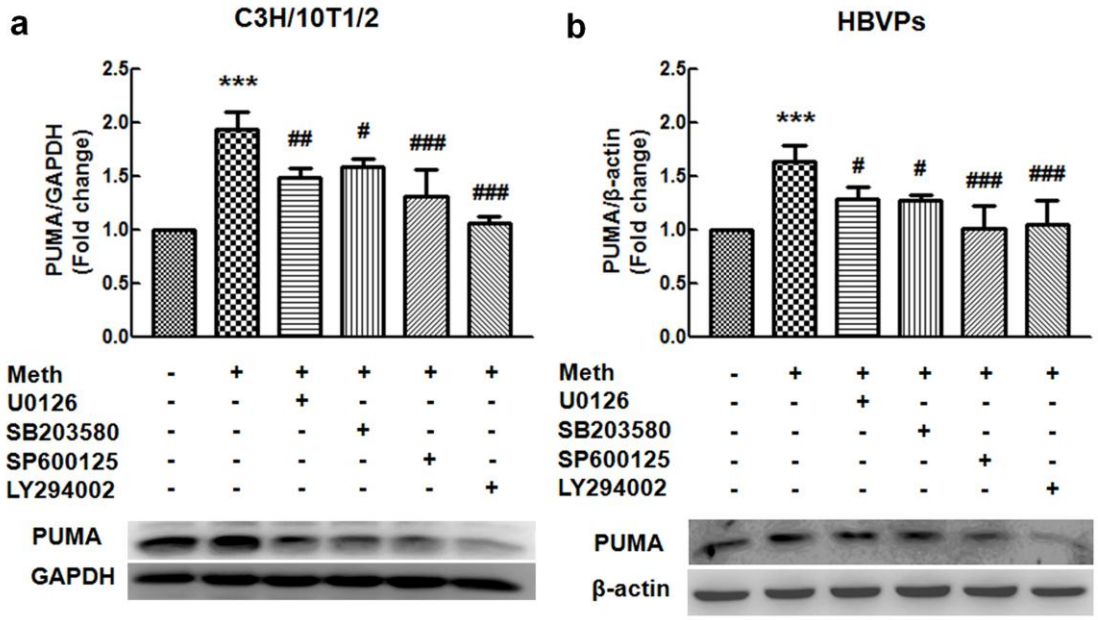

Fig 5

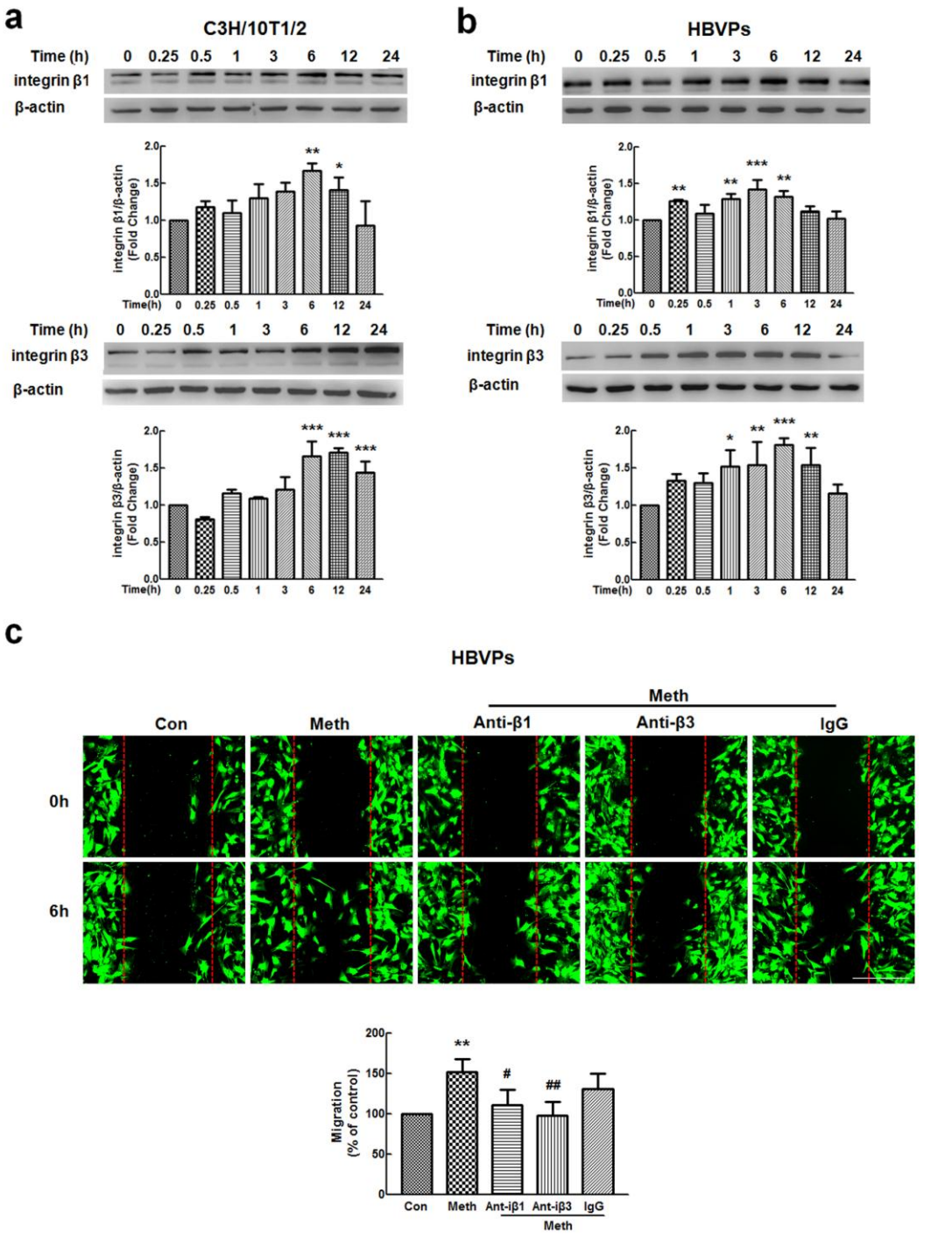
a
C3H/10T1/2
Time (h) 0 0.25 0.5 1 3 6 12 24
integrin β1
β-actin
integrin β1/β-actin (Fold Change)
Time(h) 0 0.25 0.5 1 3 6 12 24
Time (h) 0 0.25 0.5 1 3 6 12 24
integrin β3
β-actin
integrin β3/β-actin (Fold Change)
Time(h) 0 0.25 0.5 1 3 6 12 24
b
HBVPs
Time (h) 0 0.25 0.5 1 3 6 12 24
integrin β1
β-actin
integrin β1/β-actin (Fold Change)
Time(h) 0 0.25 0.5 1 3 6 12 24
Time (h) 0 0.25 0.5 1 3 6 12 24
integrin β3
β-actin
integrin β3/β-actin (Fold Change)
Time(h) 0 0.25 0.5 1 3 6 12 24
c
HBVPs
Meth
Con
Meth
Anti-β1
Anti-β3
IgG
0h
6h
Migration (% of control)
Con
Meth
Ant-iβ1
Ant-iβ3
IgG
Meth

Fig 6

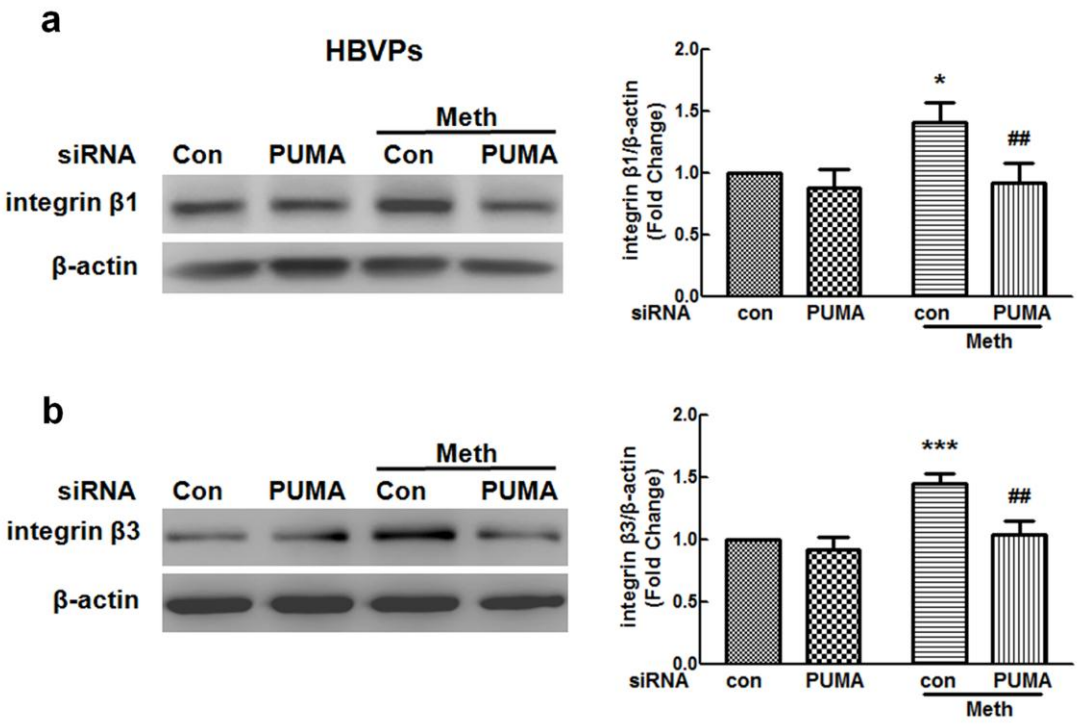

Fig 7